UC San Diego
UC San Diego Previously Published Works

Title
"Mallostery"—ligand-dependent protein misfolding enables physiological regulation by ERAD

Permalink

Journal

ISSN

Authors
Wangeline, Margaret A
Hampton, Randolph Y

Publication Date

DOI

Peer reviewed

"Mallostery"—ligand-dependent protein misfolding enables physiological regulation by ERAD

Margaret A. Wangeline[1] and Randolph Y. Hampton[2]

From the Division of Biological Sciences, the Section of Cell and Developmental Biology, University of California San Diego, La Jolla, California 92093

Edited by Phyllis I. Hanson

HMG-CoA reductase (HMGR) undergoes regulated degradation as part of feedback control of the sterol pathway. In yeast, the stability of the HMGR isozyme Hmg2 is controlled by the 20-carbon isoprenoid geranylgeranyl pyrophosphate (GGPP). Increasing GGPP levels cause more efficient degradation by the HMG-CoA reductase degradation (HRD) pathway, allowing for feedback regulation of HMGR. The HRD pathway is critical for the endoplasmic reticulum (ER)-associated degradation (ERAD) of misfolded ER proteins. Here, we have explored GGPP's role in HRD-dependent Hmg2 degradation. We found that GGPP potently regulates Hmg2 levels *in vivo* and causes reversible Hmg2 misfolding at nanomolar concentrations *in vitro*. These GGPP-mediated effects were absent in several stabilized or non-regulated Hmg2 mutants. Consistent with its high potency, GGPP's effects were highly specific such that other structurally related molecules were ineffective in altering Hmg2 structure. For instance, two closely related GGPP analogues, 2F-GGPP and GGSPP, were completely inactive at all concentrations tested. Furthermore, GGSPP antagonized GGPP's effects *in vivo* and *in vitro*. Chemical chaperones reversed GGPP's effects on Hmg2 structure and degradation, suggesting that GGPP causes selective Hmg2 misfolding. These results indicate that GGPP functions in a manner similar to an allosteric ligand, causing Hmg2 misfolding through interaction with a reversible, specific binding site. Consistent with this, the Hmg2 protein formed multimers, typical of allosteric proteins. We propose that this "allosteric misfolding," or *mallostery*, observed here for Hmg2 may be a widely used tactic of biological regulation with potential for development of therapeutic small molecules that induce selective misfolding.

Protein quality control includes a variety of mechanisms to ensure tolerably low levels of misfolded proteins in the living cell. Among these, selective degradation of misfolded, damaged, or unpartnered proteins is often employed for removal of these potentially toxic species. One of the best characterized pathways of degradative quality control is endoplasmic reticulum (ER)[3]-associated degradation (ERAD), entailing a group of ubiquitin-mediated pathways that degrade both lumenal and integral membrane proteins of the ER (1–4). All degradative quality control pathways show a remarkable juxtaposition in their action. They are all highly specific for misfolded versions of the substrate proteins, but they recognize a wide variety of distinct and unrelated substrates (5, 6). This "broad selectivity" is based on the ability of the ubiquitination enzymes to recognize or respond to specific structural hallmarks of misfolding shared by a wide variety of client substrates. The details and restrictions of these recognition features are still being discovered due to the apparently wide range of ways that E3 ligases can detect their clients (5, 7–9).

The remarkable selectivity for misfolded proteins positions degradative quality control as a powerful tool for physiological control of normal proteins. It is now clear that a number of cases exist where a normal protein can enter a *bona fide* quality control pathway to bring about its physiological regulation (10–16). The best studied example of this sort of control is the regulated degradation of HMG-CoA reductase (HMGR), a rate-limiting enzyme of the sterol synthetic pathway. In both mammals and yeast, this essential enzyme undergoes regulated degradation in response to molecular signals from the sterol pathway as a mode of feedback control of sterol synthesis. In both cases, ERAD pathways are employed to bring about the regulated degradation of the normal enzyme, allowing for a deep understanding of selectivity in ERAD and holding the promise for development of new strategies to control the levels of individual protein targets.

Our studies of sterol regulation in *Saccharomyces cerevisiae* show that the HRD ERAD pathway mediates the regulated degradation of the Hmg2 isozyme of HMGR. The HRD pathway is centrally involved in mitigating ER stress through ubiquitin-

[3] The abbreviations used are: ER, endoplasmic reticulum; HMG, 3-hydroxy-3-methylglutaryl; HMGR, HMG-CoA reductase; GGPP, geranylgeranyl pyrophosphate; HRD, HMG-CoA reductase degradation; ERAD, ER-associated degradation; 2F-GGPP, 2-fluoro-GGPP; GGSPP, S-thiolo-GGPP; FPP, farnesyl pyrophosphate; GGOH, geranylgeraniol; IPP, isopentenyl pyrophosphate; GPP, geranyl pyrophosphate; FOH, farnesol; YPD, yeast extract-peptone-dextrose; USB, urea sample buffer; IP, immunoprecipitation; IPB, IP buffer with detergent; TM, transmembrane.

mediated degradation of a wide variety of misfolded, ER-resident lumenal and integral membrane proteins (12, 17–19). The primary signal for Hmg2 degradation is the 20-carbon sterol pathway product geranylgeranyl pyrophosphate (GGPP) (Fig. 1A), which is produced during normal cell anabolism and is thus a fiduciary indicator of sterol pathway activity (20). When levels of GGPP are high, HRD-dependent degradation of Hmg2 increases, and when GGPP levels are low, Hmg2 becomes more stable, thus effecting feedback control at the level of enzyme stability. It was initially surprising that the broadly used HRD quality control pathway is required for the precisely regulated degradation of normal Hmg2. Because the HRD pathway functions to remove misfolding proteins, we had previously posited that GGPP functions by promoting a change in the structure of Hmg2 to a better HRD pathway substrate, thus employing the selectivity of the HRD machinery for purposes of physiological regulation. The studies herein test and explore that idea.

We found that GGPP directly influenced the structure of the Hmg2 multispanning anchor, in the low- to mid-nanomolar range. These potent actions of GGPP were highly specific and in fact were antagonized by a close GGPP analogue both *in vivo* and *in vitro*. Furthermore, the effects of GGPP were blocked by a variety of chemical chaperones, indicating that this molecule causes remediable misfolding of the Hmg2 structure to promote HRD recognition. Taken together, these studies led to a natural model of regulated quality control as a form of allostery that may be widely employed in biology to harness the intrinsic specificity of the many branches of degradative quality control. Because this axis of regulation appears to be based on reversible misfolding due to specific ligand binding, we have given it the name "mallostery" to reflect both the elements of misfolding implied by the prefix and the action of a selective regulatory ligand that hallmarks allosteric control of many enzymes and other proteins. This intriguing interface between quality control and protein regulation appears to be a common theme in eukaryotic regulation of various sterol-related processes (21).

Results

Specificity and potency of isoprenoids that stimulate Hmg2 degradation

In our earlier work, we tested the effects of a variety of sterol pathway molecules on Hmg2 stability (20, 22). We found that only the 20-carbon isoprenoid GGPP caused Hmg2 degradation *in vivo* when added to culture medium (20). This surprising ability of exogenous GGPP to stimulate Hmg2 degradation has been a useful feature for study of this regulatory signal (23, 24). Because this response is part of a selective negative feedback loop, we posited that the GGPP signal would be specific, physiologically relevant, and highly potent. To more systematically evaluate these ideas, we first performed dose-response experiments on pathway isoprenoids alone and in combination.

We examined the effects of candidate isoprenoids on Hmg2 stability *in vivo* using flow cytometry on cells expressing Hmg2-GFP, which undergoes regulated degradation identical to the native enzyme (25) but provides no additional enzymatic contribution to signal production. Each was tested at a variety of concentrations by direct addition to yeast cultures followed by

a 1-h incubation and flow cytometry. GGPP caused Hmg2-GFP degradation at culture concentrations as low as 1 μM, reaching a maximum at ~20 μM (Fig. 1C). The effect of GGPP on Hmg2-GFP was highly specific: the 15-carbon farnesyl pyrophosphate (FPP) and the nonphosphorylated 20-carbon geranylgeraniol (GGOH) had no effect *in vivo*. Similarly, neither of the earlier pathway isoprenoids, isopentenyl pyrophosphate (IPP) or geranyl pyrophosphate (GPP), had any effect on Hmg2-GFP at concentrations up to 27 μM. Because GGPP is synthesized by addition of the 5 carbon IPP (Fig. 1A) to FPP, we also tested whether addition of both FPP and either of the interconvertible precursors might simulate direct addition of GGPP by allowing synthesis of this regulator from these precursors. Accordingly, we also treated cells simultaneously with the combination of IPP and FPP or GPP and FPP. Neither of these coadditions had any effect.

These results indicated a clear structure-function relationship for GGPP as a degradation signal because similar molecules did not act to stimulate Hmg2 degradation. We were curious how stringent the structural features of GGPP were, so we next tested two close analogues of GGPP, 2-fluoro-GGPP (2F-GGPP) and S-thiolo-GGPP (GGSPP) (see Fig. 3A). Despite the striking similarity to GGPP, neither of these molecules stimulated Hmg2 degradation *in vivo* at even very high concentrations. Thus, the *in vivo* effect of GGPP on Hmg2 degradation appeared to be highly specific. The high specificity of GGPP in the *in vivo* assay could have a variety of explanations, so we turned to our previously employed *in vitro* assay to directly evaluate the action of GGPP on regulated stability of Hmg2.

In vitro analysis of GGPP action on Hmg2

Our early studies described a limited proteolysis assay for studying the effects of small molecules and expressed proteins on the structure of the Hmg2 transmembrane domain (26, 27). The assay uses myc_L-Hmg2-GFP, a version of Hmg2-GFP with an added single myc tag inserted into the first luminal loop of the transmembrane domain (Fig. 2A). The exact placement of the lumenal tag along the Hmg2 sequence provides two key features. First, it does not perturb *in vivo* regulation of the resulting protein. Second, because the myc tag is present in the lumenal space, complete proteolysis of the tagged Hmg2 can be accomplished by addition of proteases to the cytoplasmic side of ER-derived microsomes without loss of myc signal (26). Because ER microsomes from yeast are almost completely cytosol-side-out (28), expression of myc_L-Hmg2-GFP allows facile analysis of structural features of microsomal Hmg2-GFP with a simple limited proteolysis assay (23, 26, 27, 29).

When microsomes isolated from cells expressing myc_L-Hmg2-GFP are treated with a low concentration of trypsin, immunoblotting the protected myc epitope after SDS-PAGE reveals a characteristic time-dependent pattern of proteolyzed fragment production (Fig. 2B). Because the myc tag is protected, the total myc immunoblotting signal intensity remains unchanged. We developed this assay to explore how signals from the sterol pathway affect the structure of Hmg2 to render it more susceptible to the HRD quality control pathway (27). In those early studies, we found that the rate of myc_L-Hmg2-GFP proteolysis was altered by manipulations that affect the *in vivo*
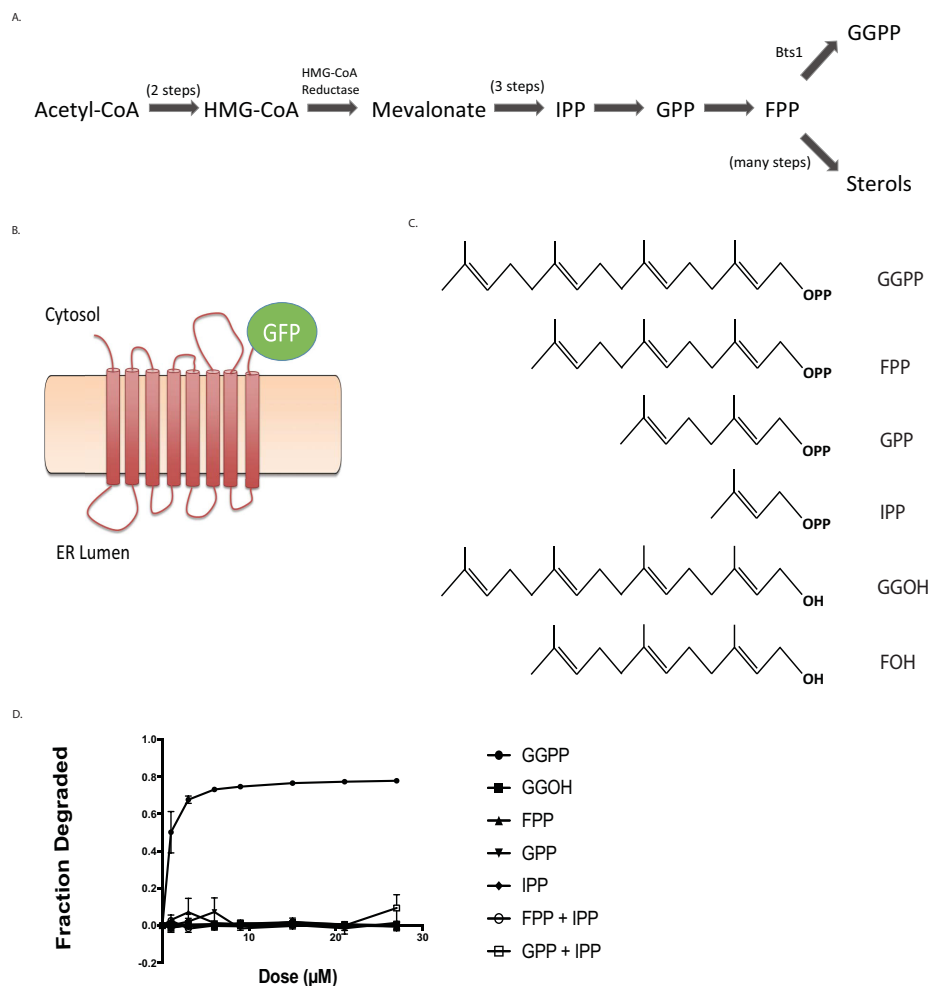
Figure 1. Effect of GGPP and related molecules on *in vivo* Hmg2-GFP degradation. *A*, schematic of the basic sterol biosynthetic pathway, showing relative positions of GGPP and other molecules mentioned in the studies. *B*, representation of Hmg2-GFP, a multispanning integral membrane ER protein and HRD pathway substrate. Hmg2-GFP undergoes normal regulated degradation but has no catalytic activity. In this construct, GFP replaces the C-terminal cytoplasmic catalytic domain. *C*, structures of key isoprenoid molecules studied in this work, including the potent biological regulator of Hmg2, GGPP. *D*, dose-response curve of the molecules pictured in *C* for stimulating Hmg2-GFP degradation, indicated by loss of *in vivo* fluorescence after a 1-h 30 °C incubation after direct addition of the indicated compounds to culture medium followed by flow cytometry, counting 10,000 cells. Fractional degradation is the difference in fluorescence initially *versus* 1 h as a fraction of initial fluorescence. Values shown are means from three experiments. *Error bars* are S.E.

stability of the protein such that *in vitro* proteolysis occurred more rapidly when microsomes were prepared from strains where the degradation signals are high (27). *In vivo*, Hmg2 or Hmg2-GFP is strongly stabilized by chemical chaperones (30). Similarly, proteolysis of microsomal myc_L-Hmg2-GFP is drastically slowed by addition of the chemical chaperone glycerol, and this structural change is fully reversible (26). We employed this *in vitro* structural assay to explore the possibility that sterol pathway signals directly affected the structure of Hmg2 to allow regulated degradation. In those studies, we showed that the 15-carbon neutral isoprenoid farnesol (FOH) caused significant acceleration of *in vitro* myc_L-Hmg2-GFP trypsinolysis, again preserving the cleavage pattern but altering the kinetics (27). This effect of FOH is fully reversible. Furthermore, mutants of Hmg2-GFP that do not respond to *in vivo* degradation signals, including a substitution of a small number of amino acids known as "TYFSA" and a single point mutant, S215A, of a highly conserved residue of the sterol-sensing domain, do not respond to farnesol in the limited proteolysis assay (23, 27). Although those results were intriguing and biologically appro-

priate, the biological role of farnesol *per se* was unclear. Although there was a clear structure-activity relationship for farnesol in the proteolysis assay, the concentrations required to cause the *in vitro* effects were very high (EC$_{50}$ ∼ 100 μM), and farnesol is extremely toxic to yeast. In the time since these studies, we discovered that the *bona fide* physiological regulator was the normally made isoprenoid GGPP, which also causes the structural transition of Hmg2-GFP in the proteolysis assay (20). Accordingly, we returned to this assay to evaluate the specificity and potency of GGPP in a more controlled setting.

In striking contrast to FOH, we found that GGPP was a potent modifier of Hmg2 structure. GGPP accelerated *in vitro* trypsinolysis at concentrations as low as ∼15 nM with an apparent half-maximum concentration lower than 200 nM (Fig. 2, *C*, *left*, and *E*). Intriguingly, this concentration is in the range of the K_m of yeast enzymes that use GGPP as a substrate (31–33), indicating that this concentration is likely physiologically relevant because the enzymes are "tuned" to concentrations of substrate that exist in their milieu. The maximal effect of GGPP was similar to that seen with the largest effects of FOH reported
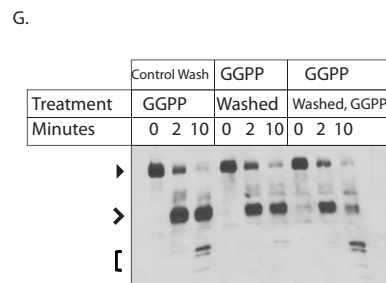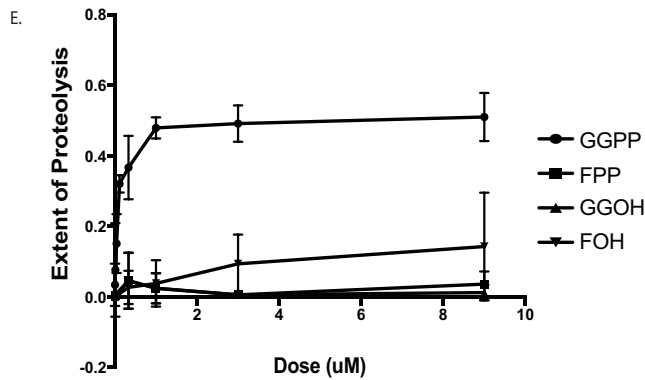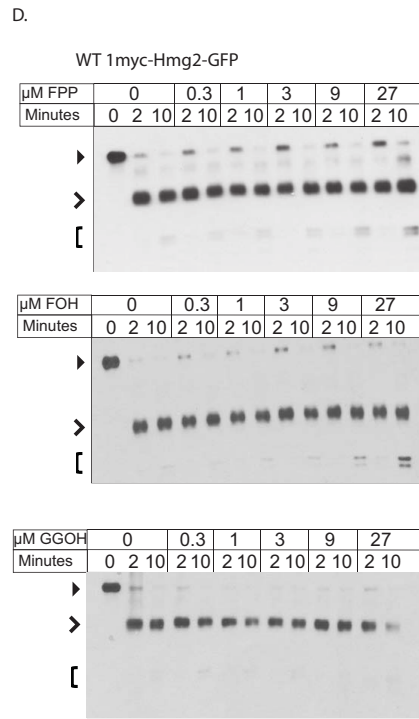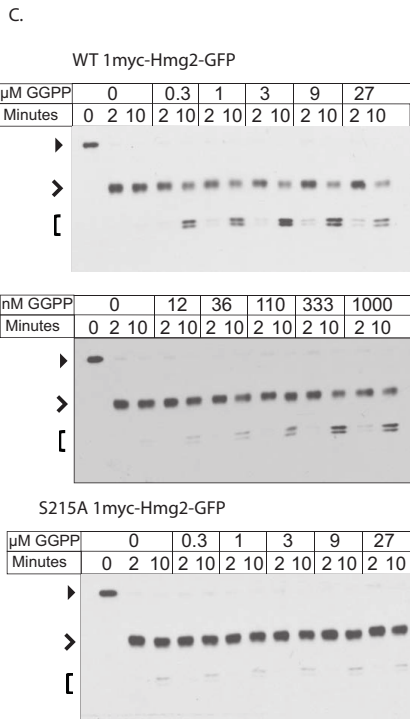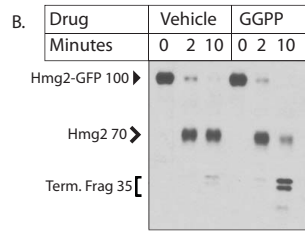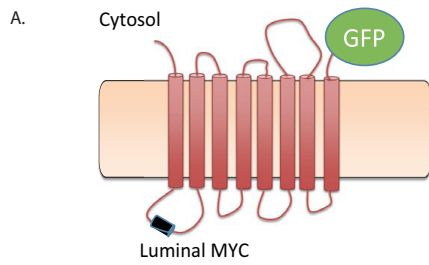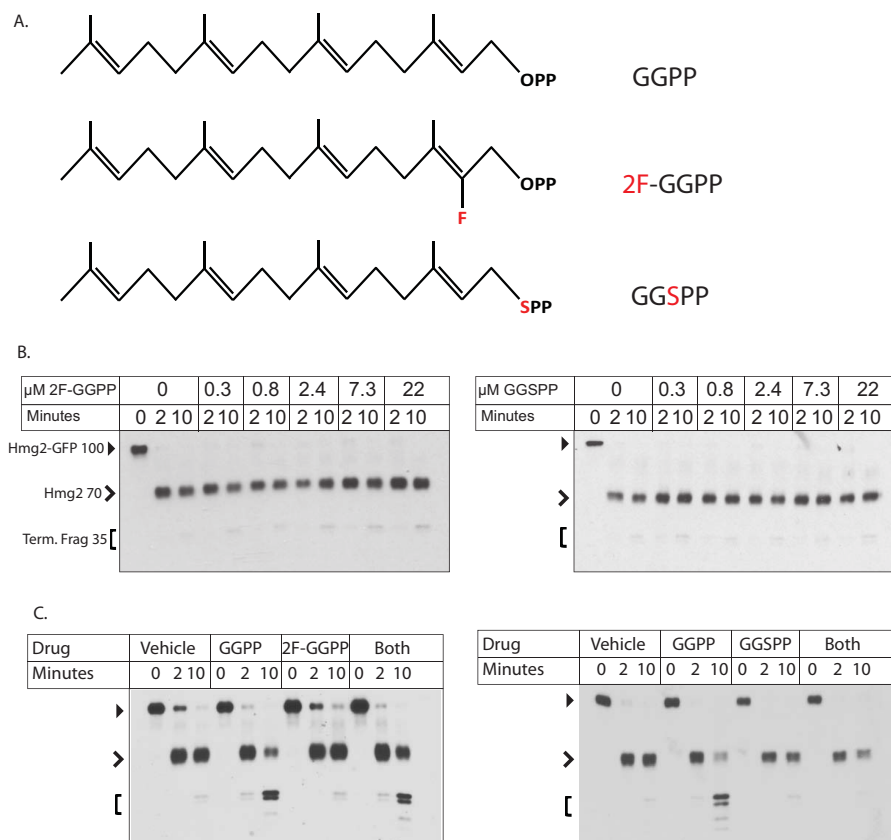
Figure 3. Inactive and antagonistic analogues of GGPP in Hmg2 structural assay. *A*, structures of GGPP, 2F-GGPP, and GGSPP, tested for activity and antagonism in this figure. Note the identical 20-carbon lipid groups of each. *B*, dose response of the two inactive GGPP analogues in the limited proteolysis assay. Full-length myc$_L$-Hmg2-GFP has a mobility of ~100 kDa (*closed arrowhead*), whereas the initial cleavage generates a transmembrane fragment of ~70 kDa (*open arrowhead*). The smaller doublets run at ~35 kDa (*Term. Frag*; *bracket*). Note that neither compound had any effect even at the highest concentration tested (22 μM). Control GGPP experiments are shown in Fig. S1. *C*, test of each inactive GGPP analogue for antagonism of the GGPP effect in the limited proteolysis assay. In both panels, 3 μM GGPP was added where indicated along with a 44 μM concentration of the indicated analogue. Microsomes were tested for effects of no addition, addition of each molecule, or the simultaneous addition of GGPP and an analogue. 2F-GGPP was tested in the *left panel*, and GGSPP was tested in the *right panel*. Note that only GGSPP antagonized the effect of GGPP.

earlier, about a 5-fold increase in proteolysis rate. The highly stable mutant S215A, which does not respond to FOH in the *in vitro* assay, also did not respond to GGPP at any concentration tested (Fig. 2*C*, *bottom*).

To investigate the specificity of this potent effect of GGPP, we directly compared a variety of isoprenoid molecules, GGOH, FPP, and FOH, all of which we have previously shown accelerate *in vitro* trypsinolysis to some degree. Although all three, to varying degrees, altered Hmg2-GFP structure, their effects occurred at half-maximum concentrations over 100-

fold higher than GGPP (Fig. 2, *D* and *E*). We next tested two close structural analogues of GGPP, 2F-GGPP and GGSPP, because these were inactive in the *in vivo* assay. Even in the direct *in vitro* assay, neither analogue induced the structural transition at any concentration tested, over 40 μM (Fig. 3, *B* and *C*).

The much higher potency of GGPP compared with isoprenoid alcohols and nonhydrolyzable analogs raised the question of whether GGPP was being used to covalently modify Hmg2 or another protein in the microsome extract. The yeast gera-

Figure 2. Effect of GGPP and related molecules on Hmg2-GFP structure *in vitro*. *A*, cartoon of myc$_L$-Hmg2-GFP. Fully regulated Hmg2-GFP with protected lumenal 1myc epitope to allow limited proteolysis assay of Hmg2 structure in isolated microsomes as described below and in Ref. 26. Full-length myc$_L$-Hmg2-GFP runs at a mobility of ~100 kDa (indicated in *B* by a *closed arrowhead*). Initial cleavage by trypsin in the linker between the transmembrane domain and the cytosolic GFP generates a fragment of ~70 kDa (*open arrowhead*), whereas the smaller doublets have a mobility of ~35 kDa (*Term. Frag*; *bracket*). Similar markers are used in subsequent figures. *B*, effect of GGPP on limited proteolysis assay. 9 μM GGPP was added to microsomes immediately before incubation with trypsin followed by SDS-PAGE and myc immunoblotting as described. *C*, concentration dependence of GGPP on WT myc$_L$-Hmg2-GFP with normal transmembrane region or the highly stabile S215A point mutation in the sterol-sensing domain. *D* and *E*, effect of some other molecules on myc$_L$-Hmg2-GFP limited proteolysis. *D*, in all panels, the molecule tested and concentration range used are listed in the *upper left corner*; concentrations are indicated along the *panel top*. Note that the effect of GGPP begins at approximately 12 nM. *E*, graphical representation of results in *C* and *D*. Immunoblot films were scanned as TIFF files, and pixels were counted for total lane intensity and for the final doublets that result from extended incubation with trypsin. Extent of proteolysis = (Doublet intensity/Total intensity). Values shown are means of three experiments. *Error bars* show S.D. *F* and *G*, GGPP effect on the Hmg2-GFP structure is fully reversible, and GGPP responsiveness remains after reversal. *F*, microsomes were washed and then treated with vehicle or GGPP (groups 1 and 2) or treated with vehicle or GGPP and then washed (groups 3 and 4). All groups were then subjected to the limited proteolysis assay as described. Note that washing first did not affect the response to GGPP, whereas washing after exposure removed the effect. *G*, microsomes that were treated with GGPP and washed maintained their ability to respond to readdition of GGPP. The *left* set of microsomes was washed and then treated with GGPP (*left* group). The *middle* set was treated with GGPP and then washed, and the *right* group was treated with GGPP, washed, and then retreated with GGPP. All samples were then subjected to the limited proteolysis assay. Note that readdition of GGPP gave precisely the same response as the first addition.

nylgeranyltransferase machinery is cytosolic and thus unlikely to have activity in our washed membranes. Nevertheless, we addressed this possibility by testing whether the GGPP effect on Hmg2-GFP was readily reversible. Microsomes were prepared normally and then washed three times in reaction buffer either before or after treatment with vehicle and GGPP. When microsomes were washed before treatment with GGPP, Hmg2-GFP became more susceptible to proteolysis as usual. When microsomes were washed after treatment, GGPP's effect was reversed (Fig. 2*F*). Furthermore, the treated and then washed microsomes remained competent for the GGPP-induced structural transition: when GGPP was added back to the washed microsomes, Hmg2-GFP again became more susceptible to proteolysis and to the same extent as the original exposure (Fig. 2*G*). This high reversibility in conjunction with our earlier *in vivo* studies on GGPP indicate that GGPP acts directly on Hmg2 rather than serving as a stable modification of Hmg2 or another regulatory protein (20).

Antagonism of GGPP action in vitro and in vivo

The GGPP analogues 2F-GGPP and GGSPP had no ability to stimulate Hmg2-GFP degradation *in vivo* (Fig. 4, *A* and *C*) or to alter Hmg2-GFP structure in the limited proteolysis assay (Fig. 3*B*). The high potency and specificity of GGPP and its ability to directly and reversibly alter the structure of Hmg2-GFP made us wonder whether it acts as a ligand, causing a structural change by specific interaction with the Hmg2 transmembrane region at a particular binding site, similar to allosteric regulation of enzymes by relevant metabolites. Accordingly, we asked whether an excess of either of the highly similar, inactive analogues might antagonize the effects of GGPP. Each was tested for an ability to block the structural effect of a low concentration of GGPP by coincubation with an excess of analogue. As expected, the test doses of either analogue had no effect on myc_L-Hmg2-GFP (Fig. 3*B*). However, the presence of a 15-fold molar excess of GGSPP clearly antagonized the structural effect of GGPP. Interestingly, only one of the analogues had this effect; the 2F-GGPP was simply inactive in an identical experiment (Fig. 3*C*). This is particularly important because both molecules have very similar chemistry and amphipathicity, both being developed to block the same class of enzymes (35, 36). Nevertheless, only GGSPP antagonized the GGPP-induced structural effects on myc_L-Hmg2-GFP.

We further explored the antagonistic action of GGSPP by examining its effects on GGPP-induced Hmg2 degradation *in vivo*. Because simultaneous addition of both GGPP and GGSPP could also have interactions on the unknown influx mechanism that appears to operate in yeast, we explored the effect of the inactive analogues on the endogenous GGPP degradation signal, which we have extensively characterized (20, 25). We first simply added each analogue to a strain with sufficient flux through the sterol pathway to produce the needed GGPP signal for Hmg2-GFP degradation. Specifically, we examined the effect of addition of inactive analogue on the Hmg2-GFP levels during a 3-h incubation period. The effects of the analogues were small but consistent with the *in vitro* effects of each: 2F-GGPP had no effect, whereas the GGSPP caused a small but reproducible increase in Hmg2-GFP steady state (Fig. 4*A*, *left*),

implying that the added antagonist can block the degradation-stimulating effect of endogenous GGPP. Importantly, an identical experiment with the similarly degraded but unregulated TFYSA mutant of Hmg2-GFP showed no effect of the GGSPP antagonist on steady-state levels, indicating that its effect was due to altering the response to GGPP signal rather than effects on the HRD pathway itself (Fig. 4*A*, *right*).

To further evaluate *in vivo* antagonism, we developed a yeast strain that constitutively generates high levels of endogenous GGPP, ensuring continuous strong signal and thus as high a rate of regulated Hmg2-GFP degradation possible. Although the effect of GGPP was originally discovered by direct addition to living cultures, our studies confirmed that endogenous GGPP was responsible for regulating Hmg2 stability (20). Endogenous GGPP can be produced by several means, including through the action of the nonessential enzyme GGPP synthase, called Bts1 (37). In our previous work, we genetically manipulated the levels of Bts1 by expressing it from the strong galactose-inducible GAL1 promoter. Capitalizing on this mode of GGPP generation, we made a yeast strain that constitutively expressed Bts1 from the similarly strong TDH3 promoter to cause continuous endogenous production of high levels of GGPP. Expression of pTDH3-*BTS1* decreased steady-state Hmg2-GFP levels by about 5-fold from WT strains (Fig. 4*B*, *left*), and further addition of GGPP to culture medium did not further decrease Hmg2-GFP (Fig. 4*B*, *right*, *orange* curve), indicating that overexpressed Bts1 is producing maximally effective levels of GGPP. To confirm that the Bts1 was producing GGPP through the normal sterol pathway, we added the HMGR inhibitor lovastatin to block the normal production of the Bts1 substrates FPP and IPP. As expected, treatment with lovastatin increased Hmg2-GFP levels ~6-fold (Fig. 4*B*, *right*, *blue* curve). This constitutive high GGPP-producing strain further demonstrated the importance of GGPP in Hmg2 stability control and allowed further testing its antagonism *in vivo*. Using the pTDH3-*BTS1* strain, we again tested the effects of direct addition of the GGPP analogues on Hmg2-GFP levels *in vivo* using flow cytometry. Consistent with the result from WT cells, 2F-GGPP did not change Hmg2-GFP levels, whereas the *in vitro* GGPP antagonist GGSPP resulted in a nearly 2-fold increase Hmg2-GFP steady-state levels over the course of the incubation (Fig. 4*C*, *left*). The expression of additional Bts1 had no effects on the *in vivo* levels of the nonresponding mutant TFYSA. Again, neither analogue had any effect on this unregulated protein (Fig. 4*C*, *right*). Taken together, these results indicate that GGPP acts directly on the Hmg2 transmembrane domain using a binding site with sufficient structural selectivity to show high potency, stringent structure activity, and specific antagonism both *in vivo* and *in vitro*.

Testing GGPP as a ligand that promotes regulated misfolding

We have previously proposed the idea that regulated Hmg2 degradation entails a programmed or regulated change to a more unfolded form, thus enhancing the probability of entry into the HRD quality control pathway (23, 27, 38). This model is supported by the observed stabilization of rapidly degraded Hmg2 by the chemical chaperone glycerol. Addition of glycerol at concentrations required for chemical chaperoning (5–20%)

A.

B.

C.
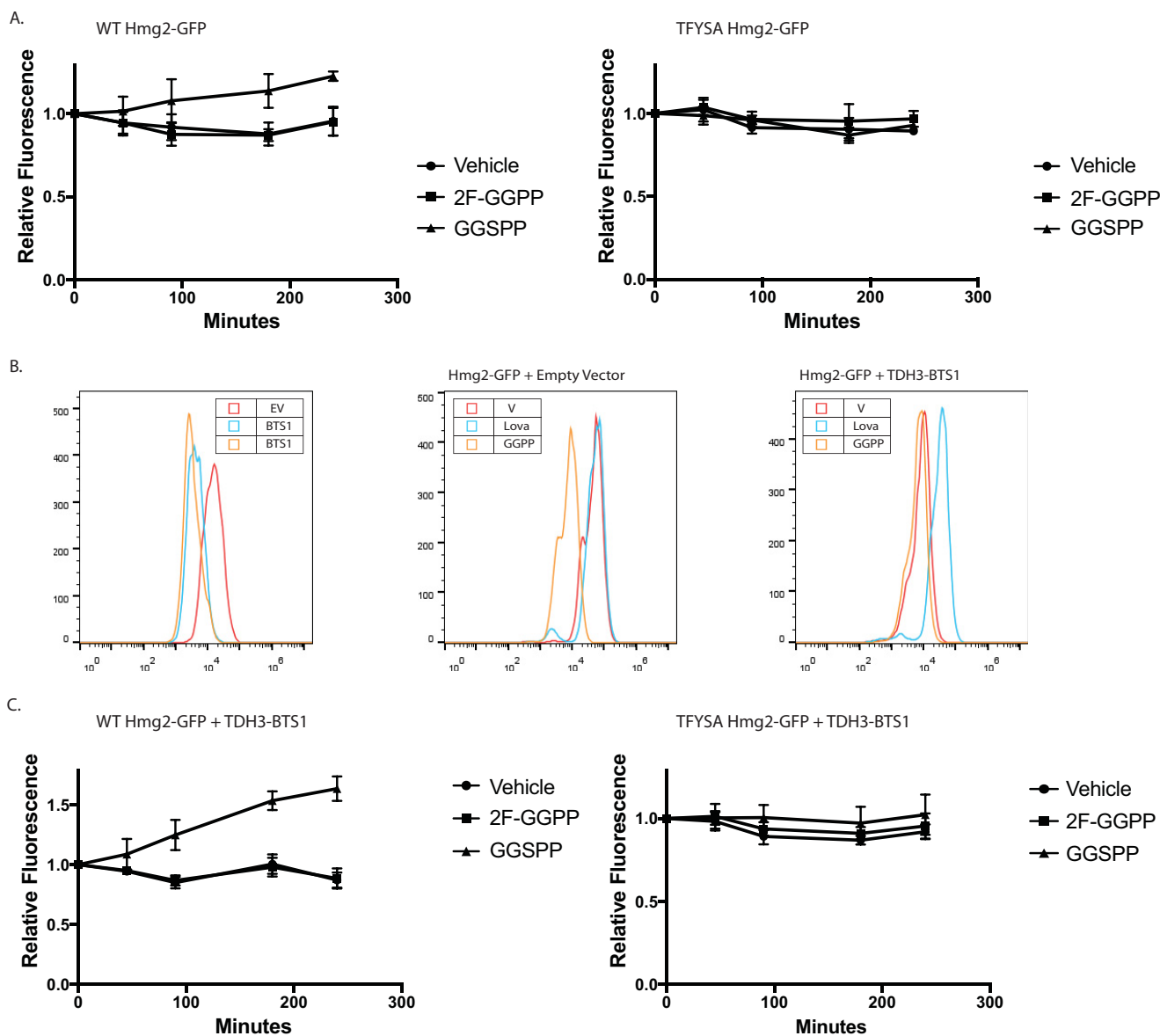
Figure 4. *In vivo* antagonism of GGPP-stimulated Hmg2-GFP degradation. *A*, effect of 2F-GGPP (nonantagonist *in vitro*) or GGSPP (antagonist *in vitro*) on WT strain with normal production of GGPP due to the sterol pathway, expressing regulated Hmg2-GFP (*left panel*) or nonregulated TYFSA mutant of Hmg2-GFP (*right panel*). All graphs show mean fluorescence from three experiments by flow cytometry of 10,000 cells each, normalized to fluorescence at time 0. *Error bars* are S.E. *B*, strains with elevated GGPP production due to strongly expressed *BTS1* gene encoding GGPP synthase. *Left panel*, steady-state fluorescence of strains expressing empty vector (*EV*; *red*) or integrated *BTS1* expression plasmid (*blue* and *orange*), showing a strong shift in the steady-state level of Hmg2-GFP fluorescence due to elevated endogenous GGPP production. *Middle panel*, effect of lovastatin (*Lova*; *blue*) or GGPP (*orange*) on Hmg2-GFP fluorescence on empty vector strain. *Right panel*, same experiment with a *BTS1*-expressing plasmid present. Note that addition of GGPP has little further effect and that lovastatin, which blocks GGPP production due to elevated Bts1, causes strong stabilization. *V*, vehicle. *C*, effect of GGPP analogues on Hmg2-GFP steady-state levels in strains with elevated GGPP production. The experiment is the same as that in *A* but with strains strongly expressing BTS1 to increase GGPP and the Hmg2-GFP degradation rate. *Left panel*, the strain expresses normally regulated Hmg2-GFP; *right panel*, the strain expresses unregulated TYFSA mutant of Hmg2-GFP.

causes rapid and reversible stabilization of Hmg2 that is undergoing *in vivo* degradation (25). Furthermore, the effect of glycerol is also observed in the limited trypsinolysis assay (26). We had previously shown that the effects of high concentrations of farnesol on Hmg2 were reversed by glycerol, consistent with the other evidence that this lipid causes selective misfolding of Hmg2. Accordingly, we tested the ability of glycerol to antagonize the effects of the highly potent GGPP-induced structural transition. First, we confirmed glycerol's effects on Hmg2 levels *in vivo*. Addition of glycerol at concentrations required for chemical chaperoning (typically 10–20%) directly to the cul-

ture medium increased Hmg2-GFP steady-state levels (Fig. 5A, *left*) and slowed the degradation rate as measured by cycloheximide chase (Fig. 5A, *right*) as expected from our earlier studies. Then, we used glycerol to evaluate the role of misfolding in the action of GGPP. When cells were treated with maximal concentrations of GGPP and subjected to cycloheximide chase, Hmg2-GFP's half-life drops from 1.5 h to ~30 min. Coaddition of glycerol partially reversed the effects of added GGPP, increasing Hmg2-GFP's half-life to over 1 h (Fig. 5B, *left*). We further tested the effect of glycerol using the *in vitro* proteolysis assay. We treated microsomes from cells expressing myc$_L$-Hmg2-
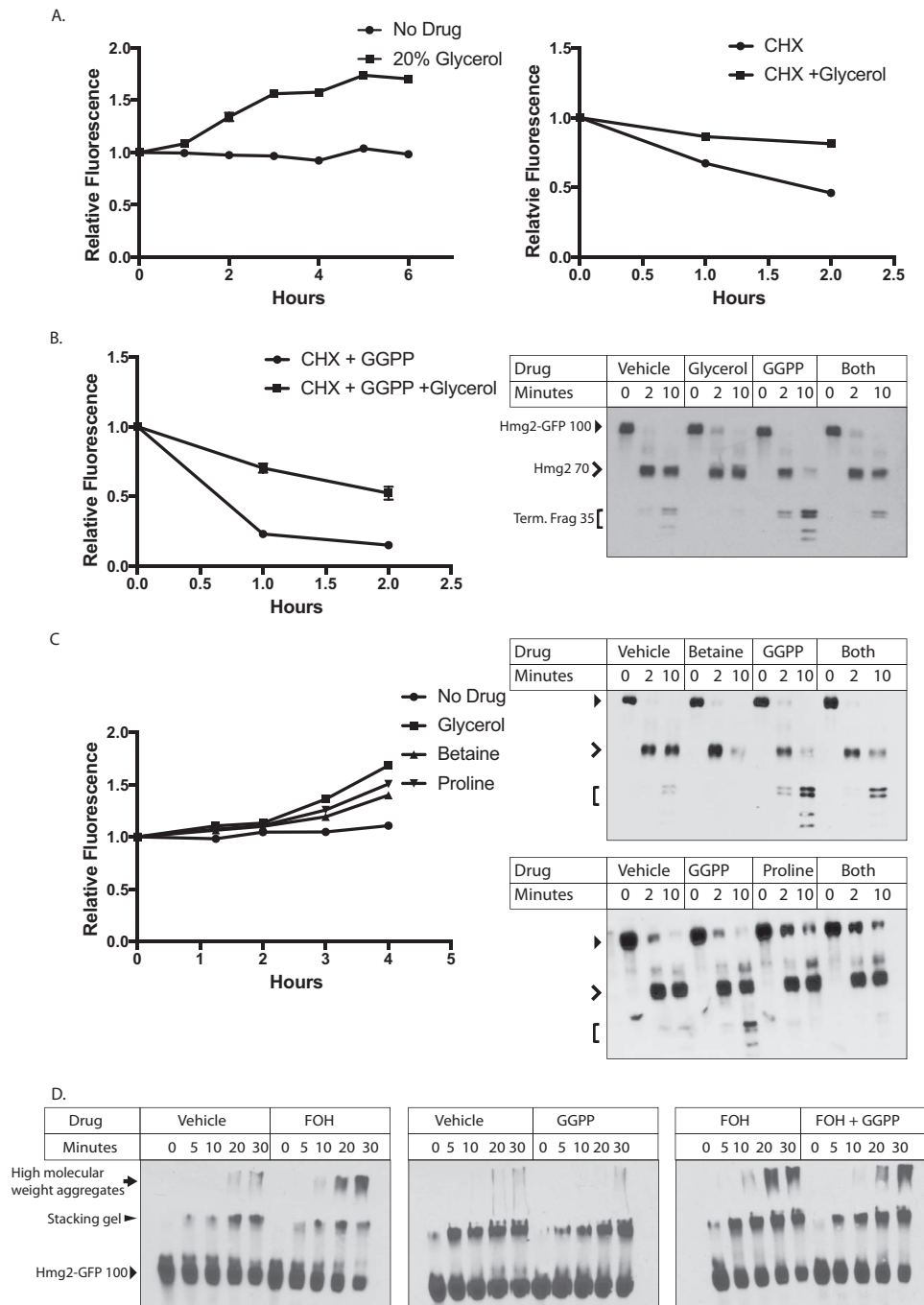
Figure 5. Effect of chemical chaperones on GGPP action *in vivo* and *in vitro*. *A*, effect of 20% glycerol on steady-state levels of Hmg2-GFP (*left*) in living cells over the indicated times after addition or the degradation rate of Hmg2-GFP (*right*) after addition of cycloheximide (*CHX*). All graphs show mean fluorescence, normalized to time 0, from three separate cultures by flow cytometry of 10,000 cells each. *Error bars* are S.E. *B*, glycerol diminished the effect of added GGPP on Hmg2-GFP degradation as measured after cycloheximide addition (*left panel*) or on Hmg2-GFP limited proteolysis due to trypsin (*right panel*). Glycerol was added to cells or microsomes immediately prior to the start of incubations. In limited proteolysis experiments, full-length myc$_L$-Hmg2-GFP runs at ∼100 kDa (indicated with a *closed arrowhead*). Initial cleavage between the cytosolic GFP and the transmembrane domain generates a transmembrane fragment of ∼70 kDa (*open arrowhead*). The smaller doublets have a mobility of ∼35 kDa (*Term. Frag; bracket*). *C*, similar effect of two other chemical chaperones, betaine and proline, on Hmg2-GFP steady state in living cells (*left panel*) or on Hmg2-GFP limited proteolysis (*right panels*) as indicated. *D*, effect of GGPP on Hmg2-GFP thermal denaturation in the presence and absence of FOH. Note that GGPP does not cause enhanced thermal denaturation of Hmg2-GFP but does mildly antagonize that caused by FOH. Full-length Hmg2-GFP has a mobility of ∼100 kDa (*solid arrowhead*). Initial higher molecular weight structures accumulate at the boundary of the stacking and resolving gels (*elongated solid arrowhead*), and high molecular weight aggregates accumulate in the stacking gel and wells (*solid arrow*).

GFP with 20% glycerol, 27 μM GGPP, or both simultaneously. As expected from earlier work with less specific signals such as FOH (27), addition of glycerol decreased the effects of added GGPP, shifting the accessibility closer to that of untreated microsomes (Fig. 5B, *right*).

These results with glycerol were consistent with GGPP causing remediable change in the folding state of Hmg2 both *in vivo* and *in vitro* and occurred at concentrations consistent with its well-known action as a chemical chaperone. To confirm this misfolding model of GGPP, we next tested the effects of two

A.

B.
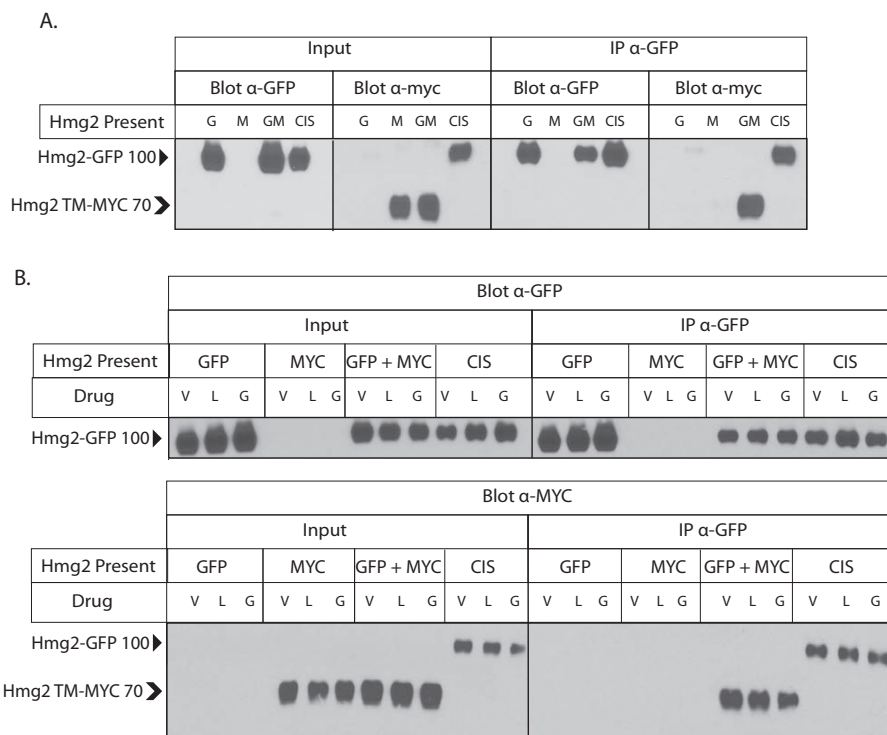
Figure 6. Hmg2 forms multimers *in vivo*. *A*, Hmg2 transmembrane regions form multimers. myc-tagged Hmg2 was coimmunoprecipitated when coexpressed with Hmg2-GFP. Microsomes from strains expressing myc-Hmg2 ("*M*"), Hmg2-GFP ("*G*"), or both ("*GM*") were solubilized with nondenaturing detergent and subjected to GPF immunoprecipitation ("*IP α-GFP*") followed by immunoblotting for GPF or myc as indicated. Inputs of 10% total lysates are shown in the *left* group ("input"). "*CIS*" is a strain that expresses a single myc-tagged Hmg2-GFP, thus putting the myc tag and GFP in cis on the same protein, as a positive control. Hmg2-GFP without any myc tag and myc$_L$-Hmg2-GFP have a mobility of ~100 kDa (indicated by a *solid arrowhead*). Hmg2 TM-MYC has a mobility of ~70 kDa (indicated by a *chevron*). The figure is spliced between anti-GFP and anti-myc sections of the panel. *B*, immunoblot showing the lack of effect of changing GGPP concentration on coprecipitation of myc-tagged Hmg2 by Hmg2-GFP. Experiments were the same as in *A* but with lovastatin pretreatment (*L*) as described to lower GGPP or with added GGPP (*G*) prior to and during immunoprecipitation to test whether altering the regulator had any effect on Hmg2 self-association. The figure is spliced between input and IP sections of each panel. *V*, vehicle; *l*, lovastatin.

entirely distinct chemical chaperones, proline and betaine. Each molecule similarly increased Hmg2-GFP levels *in vivo* (Fig. 5*D*, *left*) and reversed the effect of GGPP *in vitro* (Fig. 5*D*, *right*).

Another indicator of protein misfolding is increased susceptibility to thermal denaturation. We previously showed that treatment with high concentrations of FOH made Hmg2 more susceptible to denaturation as indicated by the formation of low-mobility electrophoretic species during brief incubation at 70 °C (27). We tested GGPP in our assay for thermal denaturation. Surprisingly, treating microsomes from a strain expressing Hmg2-GFP with GGPP at concentrations up to 20 μM did not lead to increased thermal denaturation or formation of low-mobility structures. Rather, treatment with GGPP actually slightly *decreased* thermal denaturation of Hmg2 compared with vehicle (Fig. 5*E*, *middle*). Furthermore, when microsomes were treated with both GGPP and FOH, GGPP slightly antagonized the FOH-induced denaturation, providing additional evidence for ligand binding (Fig. 5*E*, *right*). Thus, although GGPP causes an opening of the Hmg2 molecule similar to FOH and this effect is reversed by chemical chaperone treatment, the degree of Hmg2 misfolding caused by the potent and physiological GGPP signal is clearly less extreme.

Because the GGPP-caused structural transition is reversible and antagonizable, we drew an analogy to allostery. By this model, GGPP binding to a specific site would alter the structure

of Hmg2 to allow a more unfolded structure that is amenable to better recognition by the HRD machinery and reversible with chemical chaperones but is not grossly misfolded. Although allosteric transitions are usually discussed with respect to enzyme kinetics or related protein functions, it is easily conceivable that a similar alteration in structure could render a substrate more or less susceptible to engagement of quality control machinery. Nearly all allosteric proteins are multimeric, and many require this structural feature for allostery to occur (39). We tested whether Hmg2 exists as a multimer using coimmunoprecipitation, modifying our method to analyze *in vivo* interactions of Hmg2 and other proteins (24, 40, 41). Specifically, we coexpressed Hmg2 tagged with GFP and Hmg2 with a myc tag in the linker domain in the same yeast strain. Coexpressing cells were subjected to nondetergent lysis, and microsomes were prepared. Microsomes were then solubilized, and Hmg2-GFP was immunoprecipitated. When both tagged constructs were coexpressed in the same strain, immunoprecipitation of Hmg2-GFP caused coprecipitation of Hmg2 TM-MYC, demonstrating that Hmg2 forms multimeric structures (Fig. 6*A*). When only Hmg2-GFP or Hmg2 TM-MYC was expressed in a strain, we were unable to detect the other tag in input lysates or immunoprecipitations (Fig. 6*A*).

We asked whether GGPP could affect Hmg2 multimerization. We repeated the coimmunoprecipitation experiments using cells treated with lovastatin to decrease GGPP levels

Regulation by allosteric misfolding

in vivo, cells treated with added GGPP, or cells treated with only vehicle. In addition, lysis, microsome preparation, and coimmunoprecipitation from the GGPP-treated cells were all performed in the presence of added 22 μM GGPP, a concentration that maximally stimulates *in vivo* degradation and *in vitro* structural effects. In all three conditions, immunoprecipitating Hmg2-GFP pulled down the same amount of Hmg2 TM-MYC, suggesting that GGPP does not affect multimerization (Fig. 6*B*).

Taken together, these data indicate that the regulation of Hmg2 entry into the widely used and conserved HRD quality control pathway occurs by a specific and reversible interaction with the naturally produced GGPP molecule. Furthermore, the structure-activity of this interaction is stringent to the extent that closely related structures can antagonize the effects both *in vitro* and *in vivo*. A reasonable model for these data is that this represents a form of "folding allostery" by which the GGPP regulator causes a subtle structural transition to a more open or less folded state to promote physiological regulation by constitutive quality control.

Discussion

In these studies we sought to understand the GGPP-mediated regulation of Hmg2 ERAD. This included a detailed study of the structure-function features of GGPP and the effects this biological regulator had on Hmg2 itself. The emerging model is that GGPP serves as a classic allosteric regulator that, instead of reversibly changing the parameters of enzyme action, causes reversible changes in folding state to bring about physiological regulation. The potential of this mode of regulation both for basic understanding and translational implementation is high.

Using flow cytometry, we tested a variety of isoprenoid molecules for their ability to induce Hmg2 degradation *in vivo*. We also used a limited proteolysis assay of Hmg2's structure to directly examine the action of naturally occurring isoprenoids on Hmg2 structure. We found remarkable specificity for the 20-carbon isoprenoid GGPP both *in vivo* and *in vitro*. *In vivo*, GGPP was the only isoprenoid to induce Hmg2 degradation. *In vitro*, GGPP's action was both highly potent and specific. The *in vitro* effect of GGPP on Hmg2 could be observed at concentrations as low as 12 nM with a half-maximum concentration in the high nanomolar range, within an order of magnitude of the K_m of yeast enzymes which use GGPP and thus consistent with its role as a physiological indicator of mevalonate pathway activity. Other isoprenoids tested required concentrations orders of magnitude higher to induce changes in Hmg2 folding in the limited proteolysis assay.

Consistent with its high potency, we found that the effect of GGPP showed extreme structural specificity. Two close analogues of GGPP, 2F-GGPP and GGSPP, despite being very similar biophysically, had no effect on Hmg2 structure at any concentration tested. In fact, one of the inactive molecules, GGSPP, was a GGPP antagonist: GGSPP interfered with GGPP's effects on Hmg2 both *in vivo* and *in vitro*. Thus, the action of GGPP showed high potency and high specificity and was subject to inhibition by a specific antagonist analogue. Taken together, these observations suggest that GGPP controls Hmg2 ERAD by binding to a specific site on the Hmg2 transmembrane region much like an allosteric regulator of an enzyme.

We also examined the nature of Hmg2's response to GGPP. Because Hmg2 undergoes regulated entry into the HRD quality control pathway, our early studies examined whether Hmg2 undergoes regulated misfolding to make it a better HRD substrate. Consistent with this model, we showed that the chemical chaperone glycerol causes striking elevation of Hmg2 stability *in vivo* and drastically slows the rate of Hmg2 limited proteolysis (26). Those early studies showed that the 15-carbon isoprenoid molecule FOH caused Hmg2 to become less folded, and this effect of FOH was not observed with mutants of Hmg2 that do not undergo regulated degradation *in vivo* (27). The *in vitro* effect of FOH was antagonized by chemical chaperones, indicating that FOH causes Hmg2 misfolding (27). At the time of those studies, we did not know about GGPP and found FOH's specific but fairly impotent effects by direct tests *in vitro*. Accordingly, in these current studies, we explored whether the more potent and biologically active GGPP similarly caused programmed misfolding. Indeed, glycerol reversed the effects of GGPP both *in vivo* and *in vitro*. We also tested two other distinct chemical chaperones, proline and betaine. These also prevented Hmg2 *in vitro* misfolding and *in vivo* degradation upon GGPP treatment. The generality of these chemical chaperones' effects suggested that Hmg2's entry into a quality control pathway is mediated by regulated misfolding of Hmg2 in response to GGPP.

In those early studies exploring the effects of FOH on Hmg2, we also used thermal denaturation as a gauge of *in vitro* Hmg2 misfolding. Incubation of microsomes at 70 °C induced aggregation of Hmg2 into a high-molecular-weight, denatured form that remains in the stacking gel of an SDS-PAGE separation, allowing straightforward assessment of time-dependent thermal denaturation by immunoblotting (27). We showed that treatment of microsomes with high micromolar concentrations of farnesol increased the rate and extent of Hmg2 thermal denaturation, whereas mutants of Hmg2 that do not respond to FOH in the proteolysis assay also did not show effects of FOH on thermal denaturation. In contrast, GGPP did not affect Hmg2 thermal denaturation and may in fact have a slight protective effect. GGPP treatment also partially antagonized the thermal denaturation caused by farnesol. These combined results suggest that GGPP caused a subtler form of misfolding that is still remediable by chemical chaperones but not prone to enhance wholesale aggregation. In other words, GGPP action is a misfolding "sweet spot," sufficient to enhance selective degradation by the HRD machinery but not the stress-inducing and health-compromising effects of wholesale misfolding or aggregation.

Combined, these features led us to a model of "folding state allostery" in which GGPP plays the role of an allosteric ligand. Upon interacting with GGPP, Hmg2 undergoes a conformational change to a partially misfolded state that renders it more susceptible to HRD degradation. GGPP meets the criteria for ligand-like behavior: its action is specific, potent, reversible, antagonizable, and occurs at physiologically relevant concentrations. Although usually allosteric regulators are view as "agonists" of a particular structural response, antagonizing ligands are often observable in classical enzyme allostery and in fact can be part of the *bona fide* physiological control of enzyme activity

in the cell. For example, AMP activates the AMP-activated protein kinase, but ATP competes to block this activation (42, 43).

GGPP-mediated Hmg2 misfolding is sufficient to gain entry to the ERAD quality control pathway and can be reversed by treatment with several different chemical chaperones both *in vitro* and *in vivo*. However, this misfolding is not so severe as to make Hmg2 more thermally unstable and prone to aggregation. We thus propose, with admitted linguistic license, to call this structural effect mallostery, a portmanteau of the preface "mal" for misfolded or poorly structured and allostery for the nature of this regulated and physiologically useful folding transition. Although traditionally allostery has been viewed as a rigid phenomenon of highly ordered proteins, advances in structural methods have allowed for a more inclusive view. In recent years, it has been more widely recognized that allosteric regulation occurs across the whole spectrum of order in proteins, including intrinsically disordered proteins. Allostery can capitalize on disorder and misfolding with allosteric proteins undergoing disorder switching or local unfolding or becoming partially disordered upon posttranslational modification (44, 45).

Because most allosteric proteins are multimeric, we tested whether Hmg2 forms multimeric structures and found that indeed it does, but making use of coexpressed, fully regulated versions of Hmg2 with distinct epitopes. Furthermore, we found no evidence for alteration in multimerization caused by addition of even saturating concentrations of GGPP in the coimmunoprecipitation experiments. This also speaks to the idea of GGPP causing a more subtle change in structural state: full dissociation of a monomer caused by a ligand could certainly enhance recognition by the HRD pathway. However, again, it appears that the GGPP-induced effects do not take things this far down the road to structural squalor. We picture the multimeric structure as allowing a subtle alteration of folding state that can be reversed upon removal of the GGPP ligand, thus allowing quality control regulation with minimal aggregation or denaturation.

A longstanding open question about Hmg2 has been whether its regulated degradation is due to binding of a ligand or rather due to a more global biophysical processes, for example perturbation of the ER membrane by isoprenoid regulators. In this work, we found that GGPP causes Hmg2's structural transition at nanomolar concentrations, far below the concentrations that would be expected to alter phospholipid bilayers properties. Furthermore, highly similar molecules were unable to affect Hmg2 at concentrations hundreds of times higher: although <100 nM GGPP had clear effects on Hmg2 structure, 40 μM 2F-GGPP had no discernable effect. In the same vein, our prior work has found a similarly striking degree of specificity for Hmg2 itself. Single point mutations within Hmg2 render it stable *in vivo* and unable to respond to GGPP *in vitro*. The combination of stringent sequence specificity for Hmg2, structural specificity for ligand, and the high potency of GGPP make it unlikely that Hmg2 misfolding and degradation are the result of any general biophysical perturbation of the ER membrane proteome.

Another possible explanation for GGPP's action is that, by binding to Hmg2, it presents a hydrophobic patch that the quality control machinery detects as the exposed core of misfolded protein. Such so-called "greasy patches" are the basis of a strategy for artificially engineering the degradation of target proteins (46, 47). This model is at odds with two observations. One, GGPP induces not only engagement with the ubiquitin–proteasome system machinery but a structural change *in vitro*. Two, very similar (and with an identical hydrophobic tail) molecules did not cause any effects on Hmg2 *in vitro* or *in vivo*. Furthermore, GGSPP, which is nearly identical to GGPP, antagonizes GGPP's effects. This implies that GGSPP can bind at the same location as GGPP, but despite this it is unable to induce the structural transition or degradation. Were the hydrophobic end of GGPP the key to its action, one would not expect such a similar molecule to behave in the opposite manner.

This model leaves several open questions. We found that GGPP's effects on Hmg2 are specific, potent, rapid, and reversible, but does GGPP bind directly to Hmg2 and, if so, where? Are other ER proteins required for Hmg2 misfolding? It seems unlikely that there are unknown stoichiometric binding partners required for Hmg2 misfolding as Hmg2 is overexpressed in our *in vitro* experiments, but the possibility remains. Furthermore, we found that Hmg2 can be coimmunoprecipitated with differently tagged Hmg2 constructs expressed in the same cell. If Hmg2 is a multimer, does the multimerized state influence this mode of regulation? Do members of the complex influence each other in undergoing the conformational change to the misfolded state as in classical models of allostery, or are individual Hmg2s independent?

Thirty percent of the United States population suffers from dyslipidemia; more have dyslipidemia controlled by pharmaceutical treatment (48). As the rate-controlling step of the sterol pathway, HMGR is a key intervention point in metabolic disease; over 25% of adults in the United States take cholesterol-lowering medications, and over 20% take statin drugs, which target this protein (https://www.cdc.gov/nchs/data/databriefs/db226.pdf [4] and https://www.cdc.gov/nchs/data/databriefs/db177.pdf [5] (both accessed August 16, 2017)). Mammalian HMGR levels rise after statin treatment due to both increased transcription of sterol genes and stabilization of HMGR itself when sterol levels are low (51). Key components of HMGR-regulated degradation are conserved in mammals, including induction by a 20-carbon isoprenoid and ubiquitination by ER E3 ligases, including gp78, which is a Hrd1 homologue (52–55). Furthermore, when the mammalian HMGR and its ancillary regulatory proteins are expressed in insect cells, endogenous Hrd1, the same E3 ligase as in yeast, mediates sterol-regulated HMGR degradation (56, 57). These extensive similarities in the system highlight the importance of a deeper understanding of the dynamics underlying HMGR's regulated quality control degradation. A greater understanding of the

[4] M. D. Carroll, C. D. Fryar, and B. K. Kit (2011) Total and High-density Lipoprotein Cholesterol in Adults: United States, 2011–2014. Key findings data from the National Health and Nutrition Examination Survey.
[5] Q. Gu, R. Paulose-Ram, V. L. Burt, and B. K. Kit (2003) Prescription Cholesterol-lowering Medication Use in Adults Aged 40 and Over: United States, 2003–2012. Key findings data from the National Health and Nutrition Examination Survey.

underpinnings of HMGR stability may open up avenues for better targeting the pathway in human patients.

This phenomenon of ligand-programmed misfolding raises questions about more general pharmacological applications. Proteins without active sites for inhibitors to engage can be difficult to target pharmacologically and have in fact been referred to as the "undruggable proteome" (49). The ubiquitin–proteasome system has already been tapped as a tool for pharmacological targeting of these undruggable proteins through regulated degradation. Two main strategies have emerged so far: targeting proteins directly to specific E3 ligases, such as Von Hippel-Lindau protein (VHL) (50) and targeting proteins with ligands fused to a long hydrophobic molecule, or "greasy patch," to mimic a misfolded protein (47). Directing proteins to quality control through the discovery of mallosteric regulators that cause selective unfolding offers another approach for targeting the undruggable proteome; it is one that nature has clearly already discovered during evolution.

Experimental procedures

Reagents

GGPP, GGOH, FPP, FOH, GPP, IPP, and cycloheximide were purchased from Sigma-Aldrich. Lovastatin was a gift from Merck. GGSPP and 2F-GGPP were gifts from Reuben Peters (Iowa State University) and Philipp Zerbe (University of California Davis). Anti-myc 9E10 supernatant was produced from cells (CRL 1729, American Type Culture Collection) grown in RPMI 1640 medium (Gibco) with 10% fetal calf serum. Living Colors mouse anti-GFP mAb was purchased from Clontech. Polyclonal rabbit anti-GFP antibody was a gift from C. Zucker (University of California San Diego). Horseradish peroxidase–conjugated goat anti-mouse antibody was purchased from Jackson ImmunoResearch Laboratories. Protein A–Sepharose beads were purchased from Amersham Biosciences.

Yeast strains and plasmids

Yeast strains (Table S1) and plasmids (Table S2) were constructed by standard techniques. The integrating *BTS1* overexpression construct, plasmid pRH2657, was made by replacing the SpeI-SmaI fragment of pRH2654 with the Bts1-coding region amplified from pRH2477.

Yeast strains were isogenic and derived from the S288C background. Yeast strains were grown in minimal media (Difco yeast nitrogen base supplemented with necessary amino and nucleic acids) with 2% glucose or rich medium (YPD). Strains were grown at 30 °C with aeration. Lumenally myc-tagged Hmg2-GFP constructs were introduced by integration of plasmid cut with StuI at the *ura3-52* locus. The *BTS1* overexpression construct was introduced by integration of plasmid cut with PpuMI at the *leu2Δ* promoter.

Flow cytometry

Flow cytometry was performed as described previously (25, 34). Briefly, yeast strains were grown in minimal medium to early log phase ($A_{600} < 0.2$) and incubated with the indicated isoprenoid molecules (naturally occurring isoprenoid concentrations as indicated; 44 μM GGSPP and 2F-GGPP unless indi-

cated otherwise), drugs (25 μg/ml lovastatin and 50 μg/ml cycloheximide), or equal volumes of vehicle (for isoprenoid pyrophosphate molecules, 7 parts methanol to 3 parts 10 mM ammonium bicarbonate; for lovastatin, 1 part ethanol to 3 parts Tris base, pH 8; and for cycloheximide, GGOH, and FOH, DMSO) for the times indicated. Individual cell fluorescence for 10,000 cells was measured using a BD Accuri C6 flow cytometer (BD Biosciences). Data were analyzed using FlowJo software (FlowJo, LLC).

Microsome preparation

Microsomes were prepared as described previously (26). Yeast strains were grown to midlog phase in YPD. 10 OD eq were resuspended in 240 μl of lysis buffer (0.24 M sorbitol, 1 mM EDTA, 20 mM KH$_2$PO$_4$/K$_2$HPO$_4$, pH 7.5) with protease inhibitors (2 mM phenylmethylsulfonyl fluoride and 142 mM tosyl-phenylalanyl chloromethyl ketone). Acid-washed glass beads were added to the meniscus, and cells were lysed at 4 °C on a multivortexer for six 1-min intervals with 1 min on ice in between. Lysates were cleared by centrifugation in 5-s pulses until no pellet was apparent. Microsomes were pelleted from cleared lysates by centrifugation at $14,000 \times g$ for 5 min, washed once in XL buffer (1.2 M sorbitol, 5 mM EDTA, 0.1 M KH$_2$PO$_4$/K$_2$HPO$_4$, pH 7.5), and resuspended in XL buffer.

Limited proteolysis assay

Microsomes were subjected to limited proteolysis as described previously (26). Briefly, resuspended microsomes were treated with the indicated isoprenoid molecules or equal volumes of vehicle and then incubated with trypsin at a final concentration of 15 μg/ml at 30 °C. Reactions were quenched at the times indicated with an equal volume of 2× urea sample buffer (USB; 8 M urea, 4% SDS, 1 mM DTT, 125 mM Tris base, pH 6.8). Samples were resolved by 14% SDS-PAGE, transferred to nitrocellulose in 15% methanol, and blotted with 9E10 anti-myc antibody.

Thermal denaturation assay

The thermal denaturation assay was performed as described previously (27). Briefly, resuspended microsomes were treated with the indicated isoprenoid molecules or equal volumes of vehicle and transferred to PCR tubes. Samples were placed in a thermocycler (Eppendorf Mastercycler Pro) preheated at 70 °C and incubated at 70 °C for the indicated times. Samples were held on ice for 2 min prior to addition of equal volumes of 2× USB. Samples were resolved by 14% SDS-PAGE, transferred to nitrocellulose in 10% methanol, and blotted with 9E10 anti-myc antibody.

Microsome preparation for coimmunoprecipitation

Microsomes were prepared for coimmunoprecipitation as described previously (41). Yeast strains were grown to midlog phase in YPD. 10 OD eq were resuspended in 240 μl of lysis buffer with protease inhibitors (2 mM phenylmethylsulfonyl fluoride, 100 mM leupeptin hemisulfate, 76 mM pepstatin A, and 142 mM tosylphenylalanyl chloromethyl ketone). Acid-washed glass beads were added to the meniscus, and cells were lysed at 4 °C on a multivortexer for six 1-min intervals with 1 min on ice

in between. Lysates were pelleted by centrifugation in 5-s pulses until no pellet was apparent with the supernatant moved to a clean tube each time. Microsomes were pelleted from cleared lysates by centrifugation at 14,000 × *g* for 5 min, washed once in IP buffer without detergent (500 mM NaCl, 50 mM Tris base, pH 7.5), and resuspended in IP buffer with detergent (IPB; 500 mM NaCl, 50 mM Tris base, 1.5% Tween 20, pH 7.5) and protease inhibitors.

Coimmunoprecipitation

Microsomes in IPB were incubated at 4 °C for 1 h with rocking. Microsomes were pipetted up and down repeatedly, and then solutions were cleared by centrifugation at 14,000 × *g* for 15 min. Supernatants were incubated with 15 *μ*l of polyclonal rabbit anti-GFP antibody overnight at 4 °C with rocking. After overnight incubation, 100 *μ*l of a 50% protein A–Sepharose bead slurry swelled in IP buffer without detergent were added. Samples were incubated at 4 °C for 2 h with rocking. Beads were then pelleted for 30 s at low speed and 1 min by gravity and washed twice with IPB and once with IP wash buffer (100 mM NaCl, 10 mM Tris base, pH 7.5). Beads were aspirated to dryness and resuspended in 2× USB. Samples were resolved by electrophoresis on 14% polyacrylamide gels, transferred to nitrocellulose in 12% methanol buffer, and immunoblotted with anti-GFP or anti-myc antibody as indicated.

References

1. Hirsch, C., Gauss, R., Horn, S. C., Neuber, O., and Sommer, T. (2009) The ubiquitylation machinery of the endoplasmic reticulum. *Nature* **458,** 453–460 CrossRef Medline
2. Mehnert, M., Sommer, T., and Jarosch, E. (2010) ERAD ubiquitin ligases. *BioEssays* **32,** 905–913 CrossRef Medline
3. Needham, P. G., and Brodsky, J. L. (2013) How early studies on secreted and membrane protein quality control gave rise to the ER associated degradation (ERAD) pathway: the early history of ERAD. *Biochim. Biophys. Acta* **1833,** 2447–2457 CrossRef Medline
4. Smith, M. H., Ploegh, H. L., and Weissman, J. S. (2011) Road to ruin: targeting proteins for degradation in the endoplasmic reticulum. *Science* **334,** 1086–1090 CrossRef Medline
5. Brodsky, J. L., and Wojcikiewicz, R. J. (2009) Substrate-specific mediators of ER associated degradation (ERAD). *Curr. Opin. Cell Biol.* **21,** 516–521 CrossRef Medline
6. Amm, I., Sommer, T., and Wolf, D. H. (2014) Protein quality control and elimination of protein waste: the role of the ubiquitin–proteasome system. *Biochim. Biophys. Acta* **1843,** 182–196 CrossRef Medline
7. Sato, B. K., Schulz, D., Do, P. H., and Hampton, R. Y. (2009) Misfolded membrane proteins are specifically recognized by the transmembrane domain of the Hrd1p ubiquitin ligase. *Mol. Cell* **34,** 212–222 CrossRef Medline
8. Gardner, R., Cronin, S., Leader, B., Rine, J., Hampton, R., and Leder, B. (1998) Sequence determinants for regulated degradation of yeast 3-hydroxy-3-methylglutaryl-CoA reductase, an integral endoplasmic reticulum membrane protein. *Mol. Biol. Cell* **9,** 2611–2626 CrossRef Medline
9. Rosenbaum, J. C., and Gardner, R. G. (2011) How a disordered ubiquitin ligase maintains order in nuclear protein homeostasis. *Nucleus* **2,** 264–270 CrossRef Medline
10. Roitelman, J., and Simoni, R. D. (1992) Distinct sterol and nonsterol signals for the regulated degradation of 3-hydroxy-3-methylglutaryl-CoA reductase. *J. Biol. Chem.* **267,** 25264–25273 Medline
11. Sever, N., Yang, T., Brown, M. S., Goldstein, J. L., and DeBose-Boyd, R. A. (2003) Accelerated degradation of HMG CoA reductase mediated by binding of insig-1 to its sterol-sensing domain. *Mol. Cell* **11,** 25–33 CrossRef Medline
12. Hampton, R. Y., Gardner, R. G., and Rine, J. (1996) Role of 26S proteasome and HRD genes in the degradation of 3-hydroxy-3-methylglutaryl-CoA reductase, an integral endoplasmic reticulum membrane protein. *Mol. Biol. Cell.* **7,** 2029–2044 CrossRef Medline
13. Wojcikiewicz, R. J., Pearce, M. M., Sliter, D. A., and Wang, Y. (2009) When worlds collide: IP₃ receptors and the ERAD pathway. *Cell Calcium* **46,** 147–153 CrossRef Medline
14. Foresti, O., Ruggiano, A., Hannibal-Bach, H. K., Ejsing, C. S., and Carvalho, P. (2013) Sterol homeostasis requires regulated degradation of squalene monooxygenase by the ubiquitin ligase Doa10/Teb4. *Elife* **2,** e00953 CrossRef Medline
15. Gill, S., Stevenson, J., Kristiana, I., and Brown, A. J. (2011) Cholesterol-dependent degradation of squalene monooxygenase, a control point in cholesterol synthesis beyond HMG-CoA reductase. *Cell Metab.* **13,** 260–273 CrossRef Medline
16. Hampton, R. Y., and Garza, R. M. (2009) Protein quality control as a strategy for cellular regulation: lessons from ubiquitin-mediated regulation of the sterol pathway. *Chem. Rev.* **109,** 1561–1574 CrossRef Medline
17. Bordallo, J., Plemper, R. K., Finger, A., and Wolf, D. H. (1998) Der3p/Hrd1p is required for endoplasmic reticulum-associated degradation of misfolded lumenal and integral membrane proteins. *Mol. Biol. Cell* **9,** 209–222 CrossRef Medline
18. Bays, N. W., Gardner, R. G., Seelig, L. P., Joazeiro, C. A., and Hampton, R. Y. (2001) Hrd1p/Der3p is a membrane-anchored ubiquitin ligase required for ER-associated degradation. *Nat. Cell Biol.* **3,** 24–29 CrossRef Medline
19. Hiller, M. M., Finger, A., Schweiger, M., and Wolf, D. H. (1996) ER degradation of a misfolded luminal protein by the cytosolic ubiquitin-proteasome pathway. *Science* **273,** 1725–1728 CrossRef Medline
20. Garza, R. M., Tran, P. N., and Hampton, R. Y. (2009) Geranylgeranyl pyrophosphate is a potent regulator of HRD-dependent 3-hydroxy-3-methylglutaryl-CoA reductase degradation in yeast. *J. Biol. Chem.* **284,** 35368–35380 CrossRef Medline
21. Wangeline, M. A., Vashistha, N., and Hampton, R. Y. (2017) Proteostatic tactics in the strategy of sterol regulation. *Annu. Rev. Cell Dev. Biol.* **33,** 467–489 CrossRef Medline
22. Gardner, R. G., Shan, H., Matsuda, S. P., and Hampton, R. Y. (2001) An oxysterol-derived positive signal for 3-hydroxy-3-methylglutaryl-CoA reductase degradation in yeast. *J. Biol. Chem.* **276,** 8681–8694 CrossRef Medline
23. Theesfeld, C. L., Pourmand, D., Davis, T., Garza, R. M., and Hampton, R. Y. (2011) The sterol-sensing domain (SSD) directly mediates signal-regulated endoplasmic reticulum-associated degradation (ERAD) of 3-hydroxy-3-methylglutaryl (HMG)-CoA reductase isozyme Hmg2. *J. Biol. Chem.* **286,** 26298–26307 CrossRef Medline
24. Theesfeld, C. L., and Hampton, R. Y. (2013) Insulin-induced gene protein (INSIG)-dependent sterol regulation of Hmg2 endoplasmic reticulum-associated degradation (ERAD) in yeast. *J. Biol. Chem.* **288,** 8519–8530 CrossRef Medline
25. Gardner, R. G., and Hampton, R. Y. (1999) A highly conserved signal controls degradation of 3-hydroxy-3-methylglutaryl-coenzyme A (HMG-CoA) reductase in eukaryotes. *J. Biol. Chem.* **274,** 31671–31678 CrossRef Medline

ASBMB

J. Biol. Chem. (2018) 293(38) 14937–14950 **14949**

26. Shearer, A. G., and Hampton, R. Y. (2004) Structural control of endoplasmic reticulum-associated degradation: effect of chemical chaperones on 3-hydroxy-3-methylglutaryl-CoA reductase. *J. Biol. Chem.* **279,** 188–196 CrossRef Medline

27. Shearer, A. G., and Hampton, R. Y. (2005) Lipid-mediated, reversible misfolding of a sterol-sensing domain protein. *EMBO J.* **24,** 149–159 CrossRef Medline

28. Kreft, S. G., Wang, L., and Hochstrasser, M. (2006) Membrane topology of the yeast endoplasmic reticulum-localized ubiquitin ligase Doa10 and comparison with its human ortholog TEB4 (MARCH-VI). *J. Biol. Chem.* **281,** 4646–4653 CrossRef Medline

29. Flury, I., Garza, R., Shearer, A., Rosen, J., Cronin, S., and Hampton, R. Y. (2005) INSIG: a broadly conserved transmembrane chaperone for sterol-sensing domain proteins. *EMBO J.* **24,** 3917–3926 CrossRef Medline

30. Gardner, R. G., Shearer, A. G., and Hampton, R. Y. (2001) *In vivo* action of the HRD ubiquitin ligase complex: mechanisms of endoplasmic reticulum quality control and sterol regulation. *Mol. Cell. Biol.* **21,** 4276–4291 CrossRef Medline

31. Jiang, Y., Rossi, G., and Ferro-Novick, S. (1993) Bet2p and Mad2p are components of a prenyltransferase that adds geranylgeranyl onto Ypt1p and Sec4p. *Nature* **366,** 84–86 CrossRef Medline

32. Stirtan, W. G., and Poulter, C. D. (1997) Yeast protein geranylgeranyltransferase type-I: steady-state kinetics and substrate binding. *Biochemistry* **36,** 4552–4557 CrossRef Medline

33. Witter, D. J., and Poulter, C. D. (1996) Yeast geranylgeranyltransferase type-II: steady state kinetic studies of the recombinant enzyme. *Biochemistry* **35,** 10454–10463 CrossRef Medline

34. Cronin, S. R., Khoury, A., Ferry, D. K., and Hampton, R. Y. (2000) Regulation of HMG-CoA reductase degradation requires the P-type ATPase Cod1p/Spf1p. *J. Cell Biol.* **148,** 915–924 CrossRef Medline

35. Gao, Y., Honzatko, R. B., and Peters, R. J. (2012) Terpenoid synthase structures: a so far incomplete view of complex catalysis. *Nat. Prod. Rep.* **29,** 1153–1175 CrossRef Medline

36. Lin, F.-Y., Liu, C.-I., Liu, Y.-L., Zhang, Y., Wang, K., Jeng, W.-Y., Ko, T.-P., Cao, R., Wang, A. H., and Oldfield, E. (2010) Mechanism of action and inhibition of dehydrosqualene synthase. *Proc. Natl. Acad. Sci. U.S.A.* **107,** 21337–21342 CrossRef Medline

37. Jiang, Y., Proteau, P., Poulter, D., and Ferro-Novick, S. (1995) BTS1 encodes a geranylgeranyl diphosphate synthase in *Saccharomyces cerevisiae.* *J. Biol. Chem.* **270,** 21793–21799 CrossRef Medline

38. Gardner, R. G., and Hampton, R. Y. (1999) A "distributed degron" allows regulated entry into the ER degradation pathway. *EMBO J.* **18,** 5994–6004 CrossRef Medline

39. Ascenzi, P., Bocedi, A., Bolli, A., Fasano, M., Notari, S., and Polticelli, F. (2005) Allosteric modulation of monomeric proteins. *Biochem. Mol. Biol. Educ.* **33,** 169–176 CrossRef Medline

40. Vashistha, N., Neal, S. E., Singh, A., Carroll, S. M., and Hampton, R. Y. (2016) Direct and essential function for Hrd3 in ER-associated degradation. *Proc. Natl. Acad. Sci. U.S.A.* **113,** 5934–5939 CrossRef Medline

41. Neal, S., Mak, R., Bennett, E. J., and Hampton, R. (2017) A Cdc48 "retrochaperone" function is required for the solubility of retrotranslocated, integral membrane endoplasmic reticulum-associated degradation (ERAD-M) substrates. *J. Biol. Chem.* **292,** 3112–3128 CrossRef Medline

42. Gu, X., Yan, Y., Novick, S. J., Kovach, A., Goswami, D., Ke, J., Tan, M. H. E., Wang, L., Li, X., de Waal, P. W., Webb, M. R., Griffin, P. R., Xu, H. E., and Melcher, K. (2017) Deconvoluting AMP-activated protein kinase (AMPK) adenine nucleotide binding and sensing. *J. Biol. Chem.* **292,** 12653–12666 CrossRef Medline

43. Hardie, D. G. (2011) AMP-activated protein kinase: an energy sensor that regulates all aspects of cell function. *Genes Dev.* **25,** 1895–1908 CrossRef Medline

44. Liu, J., and Nussinov, R. (2016) Allostery: an overview of its history, concepts, methods, and applications. *PLoS Comput. Biol.* **12,** e1004966 CrossRef Medline

45. Nussinov, R. (2016) Introduction to protein ensembles and allostery. *Chem. Rev.* **116,** 6263–6266 CrossRef Medline

46. Lai, A. C., and Crews, C. M. (2017) Induced protein degradation: an emerging drug discovery paradigm. *Nat. Rev. Drug Discov.* **16,** 101–114 CrossRef Medline

47. Bondeson, D. P., and Crews, C. M. (2017) Targeted protein degradation by small molecules. *Annu. Rev. Pharmacol. Toxicol.* **57,** 107–123 CrossRef Medline

48. Mozaffarian, D., Benjamin, E. J., Go, A. S., Arnett, D. K., Blaha, M. J., Cushman, M., de Ferranti, S., Després, J.-P., Fullerton, H. J., Howard, V. J., Huffman, M. D., Judd, S. E., Kissela, B. M., Lackland, D. T., Lichtman, J. H., *et al.* (2015) Heart disease and stroke statistics—2015 update. *Circulation* **131,** e29–e322 CrossRef Medline

49. Crews, C. M. (2010) Targeting the undruggable proteome: the small molecules of my dreams. *Chem. Biol.* **17,** 551–555 CrossRef Medline

50. Bondeson, D. P., Mares, A., Smith, I. E., Ko, E., Campos, S., Miah, A. H., Mulholland, K. E., Routly, N., Buckley, D. L., Gustafson, J. L., Zinn, N., Grandi, P., Shimamura, S., Bergamini, G., Faelth-Savitski, M., *et al.* (2015) Catalytic *in vivo* protein knockdown by small-molecule PROTACs. *Nat. Chem. Biol.* **11,** 611–617 CrossRef Medline

51. Hwang, S., Hartman, I. Z., Calhoun, L. N., Garland, K., Young, G. A., Mitsche, M. A., McDonald, J., Xu, F., Engelking, L., and DeBose-Boyd, R. A. (2016) Contribution of accelerated degradation to feedback regulation of 3-hydroxy-3-methylglutaryl coenzyme A reductase and cholesterol metabolism in the liver. *J. Biol. Chem.* **291,** 13479–13494 CrossRef Medline

52. Jo, Y., Lee, P. C., Sguigna, P. V., and DeBose-Boyd, R. A. (2011) Sterol-induced degradation of HMG CoA reductase depends on interplay of two Insigs and two ubiquitin ligases, gp78 and Trc8. *Proc. Natl. Acad. Sci. U.S.A.* **108,** 20503–20508 CrossRef Medline

53. Song, B.-L., Sever, N., and DeBose-Boyd, R. A. (2005) Gp78, a membrane-anchored ubiquitin ligase, associates with Insig-1 and couples sterol-regulated ubiquitination to degradation of HMG CoA reductase. *Mol. Cell* **19,** 829–840 CrossRef Medline

54. Roitelman, J., and Shechter, I. (1984) Regulation of rat liver 3-hydroxy-3-methylglutaryl coenzyme A reductase. Evidence for thiol-dependent allosteric modulation of enzyme activity. *J. Biol. Chem.* **259,** 870–877 Medline

55. Sever, N., Song, B.-L., Yabe, D., Goldstein, J. L., Brown, M. S., and DeBose-Boyd, R. A. (2003) Insig-dependent ubiquitination and degradation of mammalian 3-hydroxy-3-methylglutaryl-CoA reductase stimulated by sterols and geranylgeraniol. *J. Biol. Chem.* **278,** 52479–52490 CrossRef Medline

56. Nguyen, A. D., Lee, S. H., and DeBose-Boyd, R. A. (2009) Insig-mediated, sterol-accelerated degradation of the membrane domain of hamster 3-hydroxy-3-methylglutaryl-coenzyme A reductase in insect cells. *J. Biol. Chem.* **284,** 26778–26788 CrossRef Medline

57. Faulkner, R. A., Nguyen, A. D., Jo, Y., and DeBose-Boyd, R. A. (2013) Lipid-regulated degradation of HMG-CoA reductase and Insig-1 through distinct mechanisms in insect cells. *J. Lipid Res.* **54,** 1011–1022 CrossRef Medline

≈ASBMB